Arc Furnace Modeling in ATP-EMTP

E. A. Cano Plata, *Member, IEEE*, and H. E. Tacca, *Member, IEEE*

***Abstract*[1]— The use of the arc furnace and its influence on the power system is being studied. A set of models that allows for the evaluation of the electrical behavior during steady state is presented in this paper. These models have different levels of complexity; starting by taking into account all the non-linearities of the arc furnace circuit, passing through neglecting the non-linearities of the transformer reactance and supposing that the wave shape of the voltage-current characteristic in the arc is piece–wise linear. Experimental results are presented and used to validate them.**

***Index Terms*-- Harmonics, power quality, EMTP simulation, wavelet transform, instantaneous power.**

I. Introduction

It is recognized that one of the main sources of harmonic, flicker and unbalance are found in arc furnace. These three phenomena are problems of power quality that affect our daily lives. These problems have their origins in the non linear linking of the load that is connected to the power system.

The utilities and their potential users that have this type of equipment should have a method that permits the evaluation of this type of problem.

As the behavior of the arc furnace from the electromagnetic view point is not strictly periodic, it cannot be analyzed with precision using the Fourier series and harmonics [1]. Sometimes they can be considered as transient loads for which the flicker is a greater problem than the harmonics [4]. For this reason this paper will be using the electromagnetic transient program ATP [12]. This paper will attempt to cover the study of the arc furnace from the power quality point of view and for this reason three models will be present.

First, the complete model is presented. In this model, the most important non-linearities of the arc furnace systems are represented. These are the saturation and hysteresis effect on the transformer, the power cable, and the arc phenomenon inside the furnace. An iterative method is needed to aggregate a random signal (resistance parameter) in this approximation. Then a simpler, quasi-empirical model is proposed in order to obtain an easy method to analyse the arc furnace by way of analytical expressions.

The second model is intended to be a simpler option. This simplification is achieved supposing the transformer reactance to be linear. So, the saturation and the hysteresis effect on the transformer are not taken into account in this model; then analytical expressions will be achieved and the study is quick and easy.

A deeper simplification is made with regard to the last model. The wave-shape of the arc voltage-current is supposed to be piece-wise linear and the resistance of the impedance is neglected. In this way the third approximate model is shown.

In the models special attention is paid to the current and power in the arc because they are closely related to the flicker and harmonic study.

The results for each model are compared with a real arc furnace; pqAT[2-3] is being used in order to get a validation method.

II. Arc Furnace Circuit

The main furnace elements are shown in Fig. 1. These are: Transformer reactance, power cable and arc source (the electrodes).

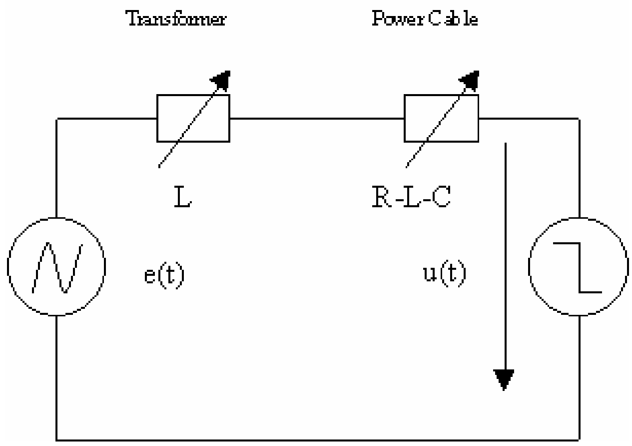

Fig 1. Arc furnace equivalent circuit.

This circuit has a strong non-linear behavior in a stationary state, as shown in Fig. 2. The arc and the oscillatory movement of the power cable are the main cause of the distorted voltage shape. Thus the cable and arc are the most important non-linearities in the circuit.

The hysteresis and the saturation in the iron core transformer are other non-linearities taken into account for the arc furnace study.

[1] This work was supported in part by the National University of Colombia and Department of Electronics, Engineering Faculty at the University of Buenos Aires.

E.A. Cano Plata is with National University of Colombia, Manizales, Colombia, A.A. 127 (e-mail: ecano@fi.uba.ar).

H. E. Tacca is with the Department of Electronic Engineering, University of Buenos Aires, Buenos Aires - Argentina, C.P. 1063, Paseo Colón 850 piso 1. (e-mail: htacca@fi.uba.ar).

Presented at the International Conference on Power Systems Transients (IPST'05) in Montreal, Canada on June 19-23, 2005
Paper No. IPST05 -067

The power cables are randomly oscillating by phase; a picture of the distorted resistance phenomena is constructed.

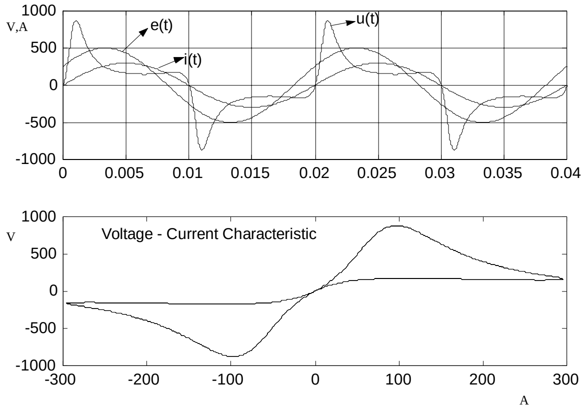

Fig. 2. Voltage and current waveforms

In the following models all parameters are obtained from the measurement on a 35MW arc furnace at 50Hz of power frequency.

III. MODEL I

In this part, the step to get a simulation method for the arc furnace is depicted by using the Mayr's model [1].

First, a description and modeling of the different elements are made. The study of reactance, power cable and arc have been emphasized, because these are the main non-linear elements.

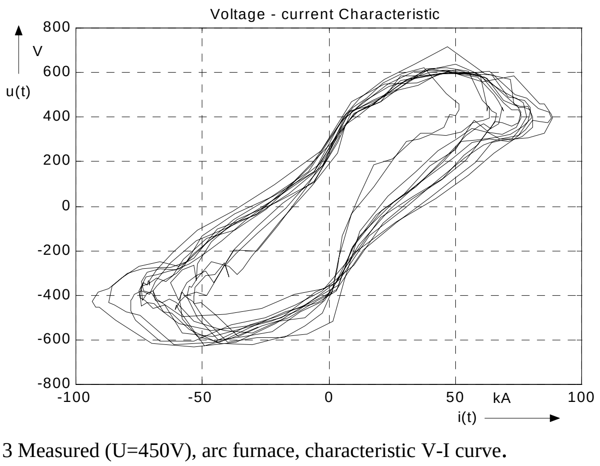

Fig. 3 Measured (U=450V), arc furnace, characteristic V-I curve.

The non-linearity prevents a direct solution from the Mayr [1] model of arc. The power in the arc is the result form of this analysis. The flicker is a derivation of the arc phenomenon and the interaction with non-linear reactance and power cable.

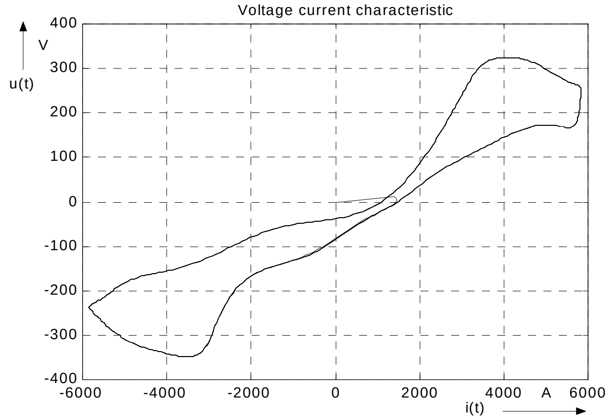

Fig. 4 Voltage-current characteristic of the arc, approximate model I.

A. *Model Description*

In this section the arc model, transformer reactance model and the power cable model are depicted, because they are the main non-linearities of the arc furnace circuit.

As is shown in Fig. 2, the arc model is derived from Mayr's model. In this way, an easy model for computer implementation is obtained.

The close form of the model shows that a current [1]:

$$i_a = \sqrt{2} I \sin \omega t \tag{1}$$

causes an arc voltage that is expressed as follows:

$$v_a = \frac{2V_0 \sin \omega t}{1 - \dfrac{\sin(2\,\omega\, t + \psi_a)}{\sqrt{1 + (2\omega \tau_a)^2}}} \tag{2}$$

where

$$V_0 = \frac{p_{r0}}{\sqrt{2} I}; \qquad \tan \psi_a = \frac{1}{2\omega \tau_a}$$

τ_a is the arc time-constant, is the most important parameter that governs the V-I characteristic, and p_{r0} the arc column power at the moment of the interruption [1].

The transformer impedance is the following non-linear element for the modeling. The model must cover the coil resistance and the saturation and hysteresis effect in the iron core. A series resistance is used to model the coil resistance (Fig. 5). The saturation effect is modeled by a non-linear inductance, and it has the following equation [5]:

$$i(t) = k_1 \phi(t) + k_2 \phi^2(t) \tag{3}$$

where $\phi(t)$ is the flux in the iron core, $i(t)$ is the current across the transformer inductance, and k_1, k_2 are constants.

Next, a resistance parallel to the non-linear inductance represents the hysteresis. Its value can be calculated from the equation [12-13]:

$$R_h = \phi_{\max} \frac{\omega_1}{d_i} \tag{4}$$

where $\phi_{\max}$ is the maximum flux, ω_1 is the fundamental frequency of the source and d_i is one half of the hysteresis width at $\phi = 0$. As a result, the model of the transformer impedance is obtained [12].

Finally, the power cable model has been included.

The transient behavior of cables has been discussed in detail in many textbooks and papers [12,13,]. ATP includes routines to compute parameters and to simulate cable transients [13].

Series impedance and shunt susceptance matrices are calculated from cable parameter computing routines based on the multi-port theory. Also, boundary conditions (like cable transposition or earth setting) may be included.

Finally, there are two options available for transient simulation: To use lumped-parameter models (cascaded π circuits) or distributed parameter models.

Simulation of cascaded π sections, computed at a fixed frequency [13], results are computationally fast. Although these models do not include frequency dependent parameters, the wanted frequency behavior is achieved by cascading the π circuit sections.

Unfortunately, lumped circuits are not good enough to model distributed parameter effects. If the particular case involves high frequencies, a greater number of π sections must be used. Then, numerical errors could appear due to great magnitude differences between the π circuit parameters and the network parameters.

When cable features affect the transient behavior of the system, the cable length and its geometry become very important.

The transient propagation speed is a function of both the inductance and the capacitance of the cable:

$$v = \frac{1}{\sqrt{LC}} m/s \quad (5)$$

where, L is inductance in henry per meter and C is capacitance in farad per meter.

The cable wave impedance is:

$$Z_o = \sqrt{\frac{L}{C}} ohms \quad (6)$$

The magnitude of the reflected wave at the electrodes depends on the reflection coefficient:

$$V_2 = V_1 \frac{Z_m - Z_o}{Z_m + Z_o} \quad (7)$$

where V_2 is the reflected voltage, V1 is the incident voltage, Z_m is the equivalent arc impedance (which depends on the arc furnace load) and Z_o is the wave impedance of the cable. In the case of multi-phase cables, these parameters must be computed for each propagation mode, using the above mentioned ATP routines.

By means of the susceptance and impedance matrices, the propagation modes may be determined by [12-14].

Eq. 7 is a simple way to understand how the transient over-voltage magnitude varies with the arc load and the installation features of the location system.

Power cable modeling in EMTP-ATP

- Cable parameter computation by Ametani routine:

In this case, impedance and susceptance matrices are computed using the multi-port theory. Boundary conditions, like cable transposition or grounding, are included.

Finally, two options for presentation are available, a set of parameters to model the cable as cascaded π circuits, or distributed parameter data to apply the Jmarti or Semlyen routines [13].

Cascaded π model

It uses the π coupled circuits of the EMTP program. Although this model does not include frequency dependent parameters, a frequency dependent behavior is achieved by the cascaded connection. However, the distributed parameter effects are not well represented by this lumped circuit model. If the particular problem involves high frequencies, a greater number of π circuits will be required. In such a case, simulation may fail due to numerical errors caused by excessive differences between the π section parameters with respect to the network parameters.

In distributed parameter models, the frequency dependence and the distributed effects of the cable parameters are taken into account [12,13]. However, the validity of these models are restricted because modal transformation matrices are assumed to be real and constant.

The effect of the random oscillation of the cable due to the electromagnetic forces in the electrodes in a three-phase arc furnace was replaced by a dynamic model in the resistance parameter.

In the case of skin effect, the resistance of the power cable was defined by a band-limited white noise variation that was defined by:

$$R_{11}(t) = R_1 + BLW \quad (8)$$

where R_1 is a constant obtained from Ametani's routine for a given geometrical cable and BLW is a band-limited (4-16Hz)[4] white noise with a zero mean.

IV. Model II

Model I will be called the Complete Model; it was present in detail for the EMTP simulation. However, the model can be simplified to achieve a fast simulation process. In model II two simplifications are made: pure sine wave three phase voltage and balanced resistive load:

First, the reactance is supposed to be linear. Thus, its model is an R-L combination, neglecting the hysteresis and saturation effects.

Second, the power cable is depreciated and a considerable increase in the resistance of the above-mentioned R-L circuit will be made.

The equivalent circuit with the above simplifications is shown in fig. 6. The source that represents the Mayr's arc model, is a time domain controlled voltage source, using TACS from ATP- Electromagnetic transients program [12].

In this case, the finer resolution levels do not allow the detection of any changes. This curve will be used as a reference in comparison with other loads in the system. It will appear as a dotted line on each of the testing cases.

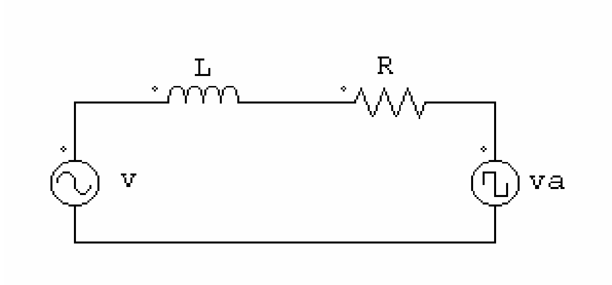

Fig.6: Approximated model II, the voltage Va is modeled using Mayr's arc, eq. (2).

Using the circuit in fig. 6, the static arc furnace model II was simulated. Fig. 7 shows the voltage-current characteristic. The power loss, represented by the enclosed area of the v-i characteristic of model II in comparison with the measurement shown by fig. 3 suggest that implementation is successful.

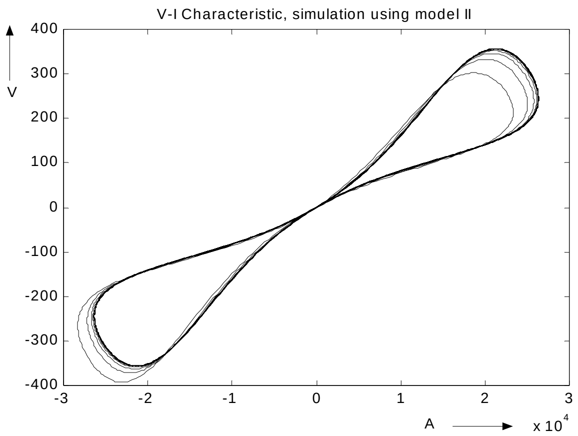

Fig. 7: Simulation obtained from model II.

For the above figure, the V-I characteristic is obtained over five full periods of the ATP simulation.

V. MODEL III

A simpler model, it was simulated using the arc furnace model proposed in [4]. This model is based on a piece-wise linear approximation of the rated v-i characteristic of the load and includes the power consumed by the arc furnace load as an input parameter. In this case, the rated v-i characteristic is altered in such a way that the power consumed by the load is that specified by the user and the thermal inertia is expressed by an exponential expression. In this way it has three regions:

$$i_1 = \frac{V_{ig}}{R_1} \tag{9}$$

$$i_2 = V_{ex} - V_{ig}\left(1 - \frac{R_2}{R_1}\right) \tag{10}$$

$$v = \begin{cases} iR_1 & 0 \le |i| \le i_1 \\ iR_2 + V_{ig}\left(1 - \dfrac{R_2}{R_1}\right), & i_1 < |i| < i_2 \\ (i_1 - i_2)e^{-|p_{ro}|t/\tau_a}, & \dfrac{d|i(t)|}{dt} < 0 \end{cases} \tag{11}$$

where V_{ex} and V_{ig} are the extinction and ignition voltage respectively, i_1 and i_2 are the currents corresponding to the ignition and extinction voltages respectively, and the thermal inertia is modeled using the last part of the Mayr's model, with the time constant τ_a in the first quadrant of the v-i characteristic shown in fig. 8

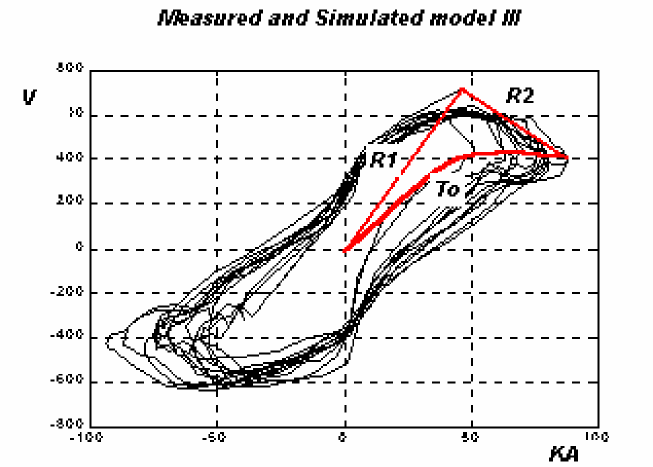

Fig 8: Measured and piece-wise linear approximation of V-I characteristic of an arc furnace load.

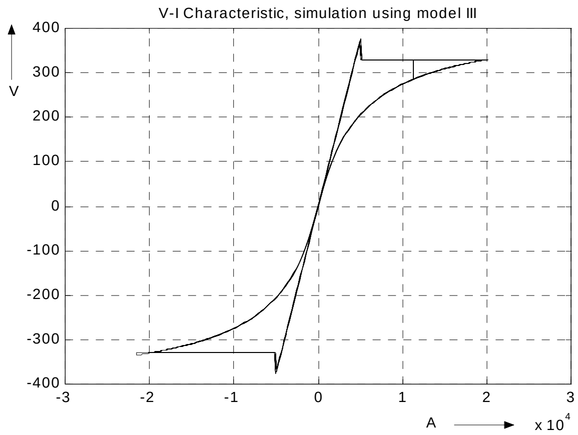

Fig. 9: V-I Characteristic obtained from simulation using arc furnace model III.

It is to be observed that the part of this model was proposed in [4]; the difference with respect to reference [4] is in the exponential delay that is typical in the plasmatic channel [1].

Fig. 9 showed the V-I characteristic in this model.

VI. Power Quality Analysis technique –pqAT-

A. Deviation Quality Index

It is defined as the noise/signal relation using the wavelets coefficient at the levels j and j_o , calculated by the multi-resolution algorithm [2,3]. The dispersion measurement with respect to a curve which represents the best of power transfer under conditions free of contamination of any kind, define the quality of the system with regard to the curve. ***Commentary:*** The standard deviation is a measurement of dispersion, which when applied to the wavelet coefficients, represents the energy of the signal, for which its mean value is zero. The dispersion of these coefficients in relation with a resistive and pure linear loads, produces a relative degree of quality. With the temporal frame in mind, the relative quality index is defined as follows :

$$Quality_k = \frac{\left|\xi_{ka}(t)-\xi_k^0(t)\right|-\left|\xi_k(t)-\xi_k^0(t)\right|}{\left|\xi_{ka}(t)-\xi_k^0(t)\right|}, \quad (12)$$

Where ξ_{ka} is the maximum admissible value for the parameter, ξ^0_k is the best trajectory and ξ_k is the measured data.

A projection of (12) in the transformed frame leads to the next definition

Definition : The particular index of the deviation of quality is defined as:

$$PDQI = \frac{sdt(d_a)-std(d_{\mathrm{Re}\,sistivo})}{std(d_a)}, \quad (13)$$

where std represents the symbol of standard deviation, d_a represents the value of the wave coefficients in level "*a*" for the power measurement on that level and $d_{Resistivo}$ represents the value of the wavelet coefficients for a power consumed by a resistive load on the same level "*a*".

This establishes an important difference with other definitions of the power quality index [6, 8, and 9].

With all this, the std_MSD curve [2-3] may be traced.

The arc furnace models are analyzed using pqAT [2] based on the following rules:

1. Measurement of v_a, v_b, v_c *and* i_a, i_b, i_c *.*

2.Transformation to i_t, v_t *in the wavelet domain.*

3. Real and imaginary power calculation [2].

4. std_MSD, the standard deviation vector formation and visualization of p, q

5. $PDQI$, *quality index deviation calculation by (13).*

B. Arc furnace Analysis

In fig. 10 and 11 the real power is measured in 25ms. The solid curve corresponds to the real system while the dotted curve corresponds to the simulated one; the approximate model I is being used. All of the models were being used with a power system of 50Hz.

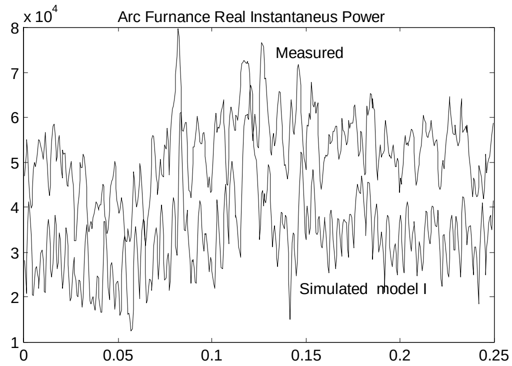

Fig. 10 Real and zero sequence power, in an arc furnace system.

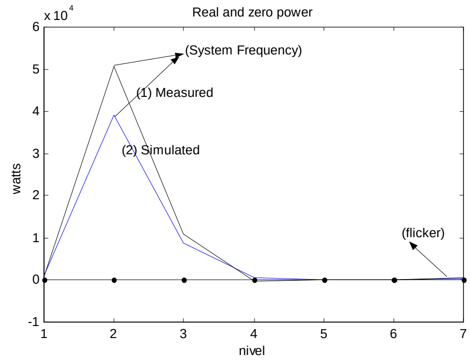

Fig. 11 Multi-resolution analysis of the real and zero sequence power.

The measured data presented in fig. 11, shows that the flicker phenomena (typical of this kind of load) is characterized at level 7 (low frequency an dc component).

The next representation shows the simplicity of the models in the simulation process using ATP. These simulations are depicted in fig. 13; it is the noise/ signal representation.

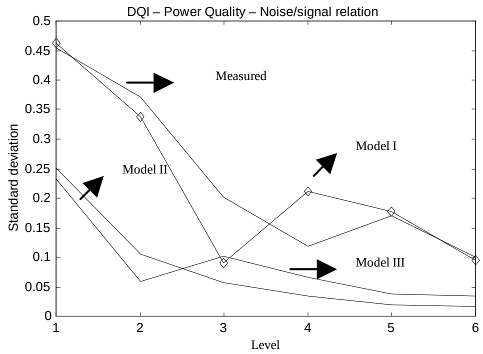

Fig. 13: std_MSD curve of each model simulated is compared with the measurement case.

VII. Conclusions

The results of measurements on a 35 MW arc furnace under the same conditions as the simulation models are included (Fig. 12 and 13).

The analysis of the simulation results presented in above figures leads to the following conclusions:

The complete Model (Model I) represents the most important representation and the instantaneous power is very close to it, as shown in Figure 11. The other models do not differ much in the power consumed, but it has a minus realistic noise/signal representation.

Every one of the models in this paper was developed using a time domain controlled voltage source in ATP. The developed load models are based on two approaches. First, one was the Mayr's arc model and the second was based on the V-I characteristic modified by a piece-wise linear and time –constant of the V-I characteristic.

Finally, PqAT was the applicator to compare the models and it proved to be successful, as shown by comparisons done between the real measured data and other models presented in a variety of simulated cases. This new method (pqAT) offers many attractive features:

The evaluation of the curve of coefficients, allows the right physical characterization of the kind of arc furnace load, which branches after the measured section.

VIII. REFERENCES

[1] A. E. Emanuel, J.A: Orr "*An Improved Method of Simulation of the Arc Voltage-Current Characteristic*", 9th international Conference on Harmonics and Quality of Power, Proceedings p.p. 148-150, October 1-4, 2000, Orlando, Florida.

[2] E.A. Cano Plata, H. Tacca "*Power Load Identification*", Journal of the Franklin Institute vol. 342, No.1, pp .97-113, January 2005.

[3] E.A. Cano Plata, H. Tacca, "*Perturbation Power*", WSEAS Trans. On Circuits and Systems vol 3, No 4, pp.996-1003, June 2004.

[4] S. Varadam, E.Makram and A. Girgis "*A New Time Domain Voltage Source Model for an Arc Furnace Using EMTP*", IEEE Transactions on Power Delivery, Vol. 11, No.3, pp. 16851691, July 1996.

[5] C.Carrillo and J.Cidrás, "*Fluorescent Lamps Modelling for Voltage Fluctuations*" ETEP.Vol. 11, No. 2.pp 119-126, March/April 2001

[6] C. Mucas, "Assessment of Electric Power Quality: Indices for Identifying Disturbing Loads", *European Transaction on Power Systems, ETEP* Vol. 8, pp. 287 – 292, July/August 1998

[7] IEEE Working Group on Non-sinusoidal Situations: Practical definitions for powers in systems with non-sinusoidal waveforms and unbalanced loads: a discussion, *IEEE Trans. on Power Delivery*, vol. 11, pp. 30-34, January 1996

[8] L.Cristaldi and A. Ferrero "A digital method for the identification of the source of distortion in electric power systems". *IEEE Trans. on Instrumentation and Measurements*, vol. .44, pp. 183-189 Feb. 1994.

[9] G. Strang and T. Nguyen, "Wavelets and Filter Banks", Wellesley-Cambridge Press, 1996,p.269.

[10] A.M. Gaouda, M.M.A. Salama, M.R. Sultan and A.Y. Chikhani, "Power quality detection and classification using wavelet-multi-resolution signal decomposition", *IEEE Trans. on Power Delivery*, vol. 14, pp. 1469-1476, October 1999.

[11] The MathWorks, MATLAB 5.3 -1999.

[12] Electromagnetic transient program (EMTP)/ATP Reference Manual. Leuven Center, Belgium, 1987.

[13] Herman Dommel, EMTP "Theory Book", MicroTran Power Systems Analysis Corporation, Vancouver, British Columbia 1996.

[14] H. Akagi, Y.Kanasawa & A. Nabae, "Instantaneous Reactive Power Conpensator Comprizing Switching Devices Without Energy Storage Components", *IEEE Trans. on Industry Applications*, Vol. IA-20, No. 3, 1984.

IX. BIOGRAPHIES

Eduardo A. Cano Plata (S'96, M'98) was born in Neiva, Colombia, in 1967. He received the B.Sc. and Specialist Engineering degree in 1990 and 1994 from National University of Colombia, Manizales, both in electrical engineering. Between 1996 and 1998 had a DAAD scholarship for postgraduate studies in electrical engineering at the National University of San Juan, Argentina. He is currently working toward the doctorate degree in engineering in the University of Buenos Aires. Since 1994 is an assistant professor at the National University of Colombia in Manizales.

Hernán E. Tacca (S'92-M'93) was born in Argentina in 1954. He received the B.E. degree in electrical engineering from the University of Buenos Aires, Argentina, in 1981, the M.S. in 1988 and the Ph.D. degree from the University of Sciences and Technologies of Lille, France, in 1993. In 1998 he received the doctorate from the University of Buenos Aires. Since 1984, he has been with the Faculty of Engineering, University of Buenos Aires, where he is currently with the Dept. of Electronics, engaged in teaching and research in the areas of industrial electronics, leading a laboratory devoted to power electronics (LABCATYP). His research interests are in the fields of SMPS, UPS, battery chargers, soft-switching techniques, and low-cost micro-controller control of power converters.